Chemical Papers (2023) 77:6111–6124
https://doi.org/10.1007/s11696-023-02925-x

ORIGINAL PAPER

Comparison of the gaseous benzene adsorption capacity by activated carbons from *Fraxinus excelsior* L. as a lignocellulosic residual

Kaan Isinkaralar[1]

Received: 18 February 2023 / Accepted: 10 June 2023 / Published online: 21 June 2023

Abstract

Benzene vapor is notoriously known to induce adverse human health, which plays a definite role in the deformation of cells. Various advanced adsorbents from lignocellulosic precursors have emerged as cheaper alternatives to the green process for the adsorption of gaseous benzene. In this paper, the prominence mainly benzene vapor removal with lignin-based adsorbent in the adsorption technology has investigated the textural, morphology, and chemical characteristics of activated carbon synthesized from *Fraxinus excelsior* L. seeds, a lignocellulosic biomass waste. Chemically starting HCl and KOH in the N_2 atmosphere was adopted, contributing to the porous carbon material's well-developed porosity and surface chemistry. Also, carbonaceous materials were investigated by Brunauer–Emmet–Teller (BET), Fourier transform infrared (FTIR), scanning electron microscopy (SEM), and X-ray diffraction. Herein, the optimum way for producing activated carbon was recognized to be: activation temperature of 800 and 700 °C in line with an impregnation weight ratio of samples to HCl 1:2 and KOH 1:3 for 2 h activation time as FE_7AC and $FE_{22}AC$, which have resulted in 676 m^2/g and 0.39 cm^3/g; 734 m^2/g and 0.48 cm^3/g of BET surface area and total pore volume, respectively. The SEM observations exhibited advanced high porosity development formed by oxidation–reduction reaction, while FTIR confirmed the presence of various surface functional groups. Moreover, benzene became more tremendously facile for four ambient temperatures (20, 25, 30, and 35 °C) and until 200 min contact time. The tremendous values varied from 96 to 224 mg/g and 122 to 286 mg/g depending on lignin-based adsorbent amounts as 0.5 or 1 g and an initial benzene concentration of 100 mg/m^3 by using FE_7AC and $FE_{22}AC$. The main innovation of this paper is exciting to assist recent paths for optimizing air filtration procedures under actual environmental circumstances, particularly regarding its compatibility with the benzene molecular structure of $FE_{22}AC$. The paper concludes that the performance of the $FE_{22}AC$ can be enhanced via improvements in its surface properties for a wide array of actual benzene concentrations from gaseous applications.

Keywords Adsorption · Biosorbent · Chemical activation · Forest residues · Gas treatment

Introduction

The rapid decline in air quality was manifested by industrialization and urbanization problems (Isinkaralar and Varol 2023; Yao et al. 2023). Exposure to benzene is the forefront and abundant volatile organic compounds (VOCs) that emerged as organic solvents in the materials and chemical contents. The growth of human societies and the development of industries lead to monomeric hydrocarbons release into the subsurface deliberately or accidentally, especially in developing countries (Isinkaralar et al. 2022; Pal et al. 2022). Continued growth in benzene emissions is a very worrying situation regarding environmental development and human health because it is onerous to decompose and can transport long distances (Liu et al. 2019; Zhao et al. 2022). Benzene, an odorous compound, can harm human health, manifesting in various dimensions with a concentration range of its environment (Chaiklieng et al. 2019; Nayek and Padhy 2020). A string of international environmental protection organizations' declarations has been widely reported to reveal benzene exposure type and concentration by Ministry for the Environment South Korea (2010), WHO (2010), ENVIRON (2014), and the Department of Environmental Health (2017) as it is a significant contributor to atmospheric

✉ Kaan Isinkaralar
kisinkaralar@kastamonu.edu.tr

[1] Department of Environmental Engineering, Faculty of Engineering and Architecture, Kastamonu University, 37150 Kastamonu, Türkiye

pollution. Here, they explained benzene exposure results in all details and even described the adventure ranging from cancer to death at long-term exposure to the ubiquitous use of benzene-containing (Sakizadeh 2019; Spatari et al. 2021). Thus, mitigating or adequately controlling the gaseous benzene, a rapidly active, tremendous substance, is essential among the VOCs.

Benzene treatments have been studied in recovery techniques. However, they still need improving from the gaseous environment, lowering process costs and safety, and the conclusions drawn from separation or/and removal have necessary implications for the development of capturing benzene molecules with several materials. In fact, definitive mechanisms to remove have already been employed, such as membrane filtration (Kim et al. 2021a), photocatalytic degradation (Luo et al. 2022), biofilters (Rene et al. 2015), catalytic oxidation (Deng et al. 2018), non-thermal plasma (Saleem et al. 2019) and adsorption (Isinkaralar 2022a, 2023a), respectively. However, an important point is the presence of benzene gas, which may increase its intensity with many factors such as indoor-outdoor environment (Sekar et al. 2019), amount of presence (Liu et al. 2020), the form of presence (gas, liquid or liquid–gas particles) (Zavala et al. 2020), whether it is single or multiple (i.e., there are other volatile organic compounds at the same time) (Fetisov et al. 2023), ambient ventilation (Brdarić et al. 2019), ambient temperature–pressure (Jang et al. 2015), and the humidity of the environment (Li et al. 2020a). In this case, it is crucial to determine the removal method of benzene, which is desired to be eliminated, by evaluating the situation and considering the conditions. The adsorption method is known to be successful in VOCs environments (nonpolar) but not in all gaseous environments (polar) (Yang et al. 2018). However, the usage network for adsorption is quite rich, more simple, cost-effective, and eco-friendly among the methods (Miller et al. 2022). When the particular application results for liquid, gas, and liquid–gas in the literature were examined, the yield was relatively high compared to other methods (Zhang et al. 2017). Although the results showed the success of the adsorption process in a promising way, they also brought different results (Kwiatkowski and Broniek 2017; Szulejko et al. 2019). At the beginning of these, a wide range of conventional adsorbent materials used regular activated carbons (ACs) (Isinkaralar 2023b), MOF (Mehralipour et al. 2022), modified ACs (Deng et al. 2021), polymeric (Long et al. 2012), carbon nanostructures (Padilla et al. 2018) for separation or analytical purposes of benzene removal. The adsorbents mentioned above have advantages as well as disadvantages that, in turn, lead to the demand, such as the scarcity of raw materials used in the production phase, their value owing to minimum operational and maintaining cost, suitability of powder-granule-particle size, variability of pore volumes, number of desorption cycles-efficiency, and the hazardous waste that arises in case of not being able to desorption (Gao et al. 2020; Quesada et al. 2020). The main point to know here is the correct selection of the application area and way with an optimum adsorbed amount. The high flow rate in industrial applications can cause higher adsorbent doses during the increased sharp fill-up to pores (González-García 2018; Pui et al. 2019). For this purpose, the high surface area and micropore volume of the produced ACs is a priority factor thanks to adequate installation or operation maintenance (Zhu et al. 2020; Zhang et al. 2022). In addition, it is vital to have suitable raw materials (abundant and cheap) and low activation costs to optimal produce in large quantities. In this case, the resulting agricultural, forestry, and farming wastes have proven themselves as appropriate raw material in the production of AC (Largitte et al. 2016; Ma et al. 2018; Franco et al. 2021). In particular, the authorities have accepted activating lignin-containing raw materials as environmentally friendly, green, and sustainable. *Fraxinus excelsior* L. are deciduous trees that have shown high production of valuable biomass for ACs production, which have been widely distributed in many geographies and have been treated in traditional medicine in different parts of the world (Flanagan et al. 2013; Isinkaralar 2023c).

In this study, it has been a priority for renewable carbon materials from seeds of *F. excelsior* for the lignocellulosic biomass and its incredible versatility of applications in benzene removal. It is aimed to obtain ACs using its seeds as a precursor. It needs the highest surface areas and pore volumes due to mixing and impregnating HCl and KOH, which are used in chemical activation at various ratios. To further clarify the physicochemical properties of ACs, this study was investigated, and the objective was to research the removal efficiency of benzene vapor at several concentrations. By comparing the yield, it has been tried to show how the effect of surface area and pore volumes could be significantly developed and utilized for benzene molecular retention. In addition, it is thought that the suitable chemicals treated into lignocellulosic material will lead to minimizing gas removal studies and inspire future VOC studies.

Materials and methods

Reagents and instruments

The lignocellulosic waste samples were collected as a forest residual during autumn from a local forest in Kastamonu, Türkiye. The proximal, ultimate, and lignocellulosic analysis seeds of *Fraxinus excelsior* L. were determined by ASTM standards. In the cumulative representation, it can be gained as its low content of ash (ASTM D 1102-84, 2013), moisture (ASTM E871-82, 2019), and high rate of volatile matter

(ASTM E872-82, 2019; ASTM 2011) indicates that the final carbonaceous *F. excelsior* seeds structure is corresponding to produce FEACs. Chemical activation of seeds was carried out with the use of hydrochloric acid (HCl) and potassium hydroxide (KOH) as activating agents, which were purchased from Merck (analytical grade). Sigma-Aldrich supplied benzene (99.8%) and BTEX mixture analytical standard, and Tenax®-TA single sorbent tubes (200 mg, 60/80 mesh Supelco, USA) were also provided from Millipore/Sigma. Nitrogen (N_2, 99.99%) and distilled water with conductivity < 1 µS/cm were also utilized in this experiment.

Post and in-situ synthesis of FEACs

The collected raw material was brought to the laboratory, and preliminary preparations for the synthesis processes were started to reduce to approximately 1 × 1 cm in size. Samples are purified abundantly and dried for one week at 45 °C to remove humidity. After making sure that it dries, it is separated into tiny particles, which are ground as the powder form. In order to eliminate the remaining moisture in the powdered samples, they were poured into a long tray, and the spread samples were mixed every hour and dried at 60 °C for 24 h. Each piece was weighed and prepared as 50 g into beakers. It was mixed with HCl at weight ratios of 1:1, 1:2, and 1:3, respectively. Meanwhile, it was heated at 100 °C for one hour with a continuous rotation of 150 rpm for 1 h. After being taken from the heater, it evaporated for a day at 105 °C. A horizontal tube reactor with a diameter of 8 cm and a height of 22 cm was utilized, accompanied by a nitrogen (N_2) flow rate of 80 mL/min as a carrier gas in a programmable furnace. At the beginning of the carbonization process, the temperature, N_2 flow, and digital indicators of the horizontal tube furnace were controlled in experiments. The solid form samples in the beaker were provided with uninterrupted pyrolysis in an N_2 environment at 600, 700, 800, and 900 °C with a heating rate of approximately 10 °C/min for 2 h. After 2 h, the furnace, left to cool without cutting the nitrogen supplied to the system, was opened after 4 h. The pH value of the activated samples obtained was neutralized by washing with 0.1 M NaOH. Then it was washed with boiling water to remove remnants and left in the oven at 105 °C to dry, then segregated using 0.45 µm of membrane filters. After performing the same procedures for KOH, it was washed with 0.1 M HCl to neutralize the pH value, then passed through the boiling water, filtered, and left in the oven at 105 °C to dry. Table 1 summarizes that a total of 24 FEACs are labeled from FE_1AC to $FE_{24}AC$ and made ready for characterization.

The FE_7AC and $FE_{22}AC$ were selected to investigation structural characteristics by BET (NOVA touch LX4, Quantachrome, USA) equation at the amount of N_2 adsorbed at the relative pressure $P/P_0 = 0.995$ for surface area calculation and DFT (density functional theory) applied to the adsorption isotherms for the pore distribution, SEM (Quanta FEG 250, FEI, USA) with 4500 × magnitude and 10.00 kV for microstructures, FTIR (Perkin-Elmer TGA 7, Waltham, MA) using the KBr disk method (100 scans, from 4000 to 450 cm^{-1}, resolution 4 cm^{-1}) for surface chemistry, elemental analysis (EuroVector, model EA3000 Single, Italy) for elemental components, TGA (STA7300, Hitachi, Japan) under nitrogen and synthetic air atmospheres in an alumina crucible (from 25 to 1000 °C and heating rate of 20 °C min^{-1}) for decomposition processes and XRD (D8 Advance, Bruker AXS Gmbh, Germany) with a CuKα radiation (40 kV, 30 mA and from 5 to 85) for determining the crystallite size and nitrogen adsorption (Quadrasorb-Tri, Quantachrome Instruments) at 77 K.

Table 1 Nomenclature of FEACs

Impregnation ratio	Activating reagents	Ambient temperature	ACs ID
1:1 (w/w)	HCl	600 °C	FE_1AC
1:1 (w/w)	HCl	700 °C	FE_2AC
1:1 (w/w)	HCl	800 °C	FE_3AC
1:1 (w/w)	HCl	900 °C	FE_4AC
1:2 (w/w)	HCl	600 °C	FE_5AC
1:2 (w/w)	HCl	700 °C	FE_6AC
1:2 (w/w)	HCl	800 °C	FE_7AC
1:2 (w/w)	HCl	900 °C	FE_8AC
1:3 (w/w)	HCl	600 °C	FE_9AC
1:3 (w/w)	HCl	700 °C	$FE_{10}AC$
1:3 (w/w)	HCl	800 °C	$FE_{11}AC$
1:3 (w/w)	HCl	900 °C	$FE_{12}AC$
1:1 (w/w)	KOH	600 °C	$FE_{13}AC$
1:1 (w/w)	KOH	700 °C	$FE_{14}AC$
1:1 (w/w)	KOH	800 °C	$FE_{15}AC$
1:1 (w/w)	KOH	900 °C	$FE_{16}AC$
1:2 (w/w)	KOH	600 °C	$FE_{17}AC$
1:2 (w/w)	KOH	700 °C	$FE_{18}AC$
1:2 (w/w)	KOH	800 °C	$FE_{19}AC$
1:2 (w/w)	KOH	900 °C	$FE_{20}AC$
1:3 (w/w)	KOH	600 °C	$FE_{21}AC$
1:3 (w/w)	KOH	700 °C	$FE_{22}AC$
1:3 (w/w)	KOH	800 °C	$FE_{23}AC$
1:3 (w/w)	KOH	900 °C	$FE_{24}AC$

Benzene adsorption measurement

Before each test, FE_7AC and $FE_{22}AC$ as carbonaceous adsorbents were separately premixed with benzene threshold concentrations from 5 to 100 mg/m^3. 0.5 and 1 g of the FE_7AC and $FE_{22}AC$ were used for each investigation. A batch reactor that allows the benzene to evaporate for sampling at

certain periods, temperature controlled, monitored the mass balance of benzene vapor is used for the experiment. It was connected to the N_2 flow rate of 50 mL/min as a carrier gas were directly collected into Tenax®-TA single sorbent tube by using a vacuum air pump (200 mL/min, AirLite 110–100, SKC, USA). Tenax tubes were analyzed using thermal desorption (TD; Markes Unity Series 2, Markes International Ltd., Llantrisant, U.K.) coupled with a gas chromatography/mass spectrometry detector (GC–MS; Thermo Scientific Trace 1300 and ISQ-QD Thermo Fisher Scientific). TG-624 capillary column (60 m × 0.25 mm ID × 1.4 µm film) for thermal desorber was inserted to check compounds based on US EPA Method TO-17 (USEPA 1999). To supply that the different test findings were calculated using Eq. (1) when FE_7AC and $FE_{22}AC$ were occasioned by the amount of FE_7AC and $FE_{22}AC$ rather than experimental errors, experiments under the same conditions were repeated at least once until reproducible results were attained.

$$q_{(mg/g)} = \left(\frac{FxC_0x10^{-9}}{W}\right)\left[\left(\frac{C_i}{C_0}xt_s\right) - \left(\int_0^{t_s}\frac{C_i}{C_0}d_t\right)\right] \quad (1)$$

where q (mg/g), F (mL/min), W (g), C_0 (mg/m^3), C_i (mg/m^3), and t_s (min) are the saturated benzene adsorption capacity, the airspeed, the weight of FEACs, initial benzene concentration, benzene output concentration, and saturation time in removal system, respectively.

Results and discussion

The different physicochemical characteristics of FEB and FEACs were determined using ASTM standards.

Porosity properties of FEACs

Table 2 demonstrates the ultimate, proximal, and lignocellulosic analysis results of the selected materials, with the corresponding yield values. Cellulose hemicellulose and lignine values of 31.50 ± 3.40, 35.80 ± 2.60 and 20.90 ± 3.80 in feedstock are the three main components of the biomass content of FEB. Also, near high volatile matter (68.53%), moisture (8.64%), and low ash content (1.12%) were found and they are dramatically lower than those of customarily used biomass materials. The carbon content of FE_7AC and $FE_{22}AC$ were obtained as 67.27 and 78.22%. A somewhat higher yield was observed by increasing that carbon amount within a wide spectrum of applications tested. However, varying the impregnation ratio from 1 to 3 did not significantly affect that respect. Still, it increased the ash content of the resulting carbon due to more residual other elements remaining after washing. The elemental composition showed for FE_7AC and $FE_{22}AC$ the carbon content as 67.27 and 78.22%, hydrogen as 4.96 and 1.34%, nitrogen as 2.83 and 0.77%, and oxygen as 21.42 and 19.21% thanks to the advantage of using lignin as the carbon precursor. It is a high grade precursor material for adsorption applications due to its high carbon content (≥ 40%), cellulose (40% to 60%), hemicellulose (20% to 40%) and lignin (10% to 25%). (Boundzanga et al. 2022; Isinkaralar and Turkyilmaz 2022; Xiang et al. 2022). Arminda et al. (2021) determined the

Table 2 The result of the analysis of starting materials

Analysis type	Parameter	Selected materials		
		FEB	FE_7AC	$FE_{22}AC$
Ultimate	C (%)	44.07	67.27	78.22
	H (%)	4.58	4.96	1.34
	O (%)	49.36	21.42	19.21
	N (%)	0.39	2.83	0.77
	Others (%)	0.60	3.52	0.46
Proximal	Moisture (%)	8.64	2.05	2.59
	Volatile substance (%)	68.53	17.26	18.93
	Fixed carbon (%)	21.29	78.53	73.48
	Ash (%)	1.12	1.21	3.10
	Others (%)	0.42	3.00	4.49
Biochemical component	Cellulose (%)	31.50 ± 3.40	n.a	n.a
	Hemicellulose (%)	35.80 ± 2.60	n.a	n.a
	Lignin (%)	20.90 ± 3.80	n.a	n.a
Yield (%)		n.a	59.50	51.80

n.a. non-available

chemical composition of untreated olive tree pruning (OTP) residues. Accordingly, cellulose hemicellulose lignin was found to be 31.88%, 17.26% and 9.26%. However, these values changed to 17.73, 2.19 and 5.93 after pretreatment. Heidarinejad et al. (2020) reviewed porous carbonaceous material and unique adsorption properties that can be accelerated depending on structure diversity. The various lignocellulosic wastes have been converted into ACs for their variable values of lignocellulosic traits.

Figure 1 displays the N_2 adsorption/desorption isotherms and the pore distributions of the FE_7AC and $FE_{22}AC$. Figure 1A exhibits the isotherms hysteresis at a high relative pressure (P/P_0), mesopores characteristics, which the adsorption branch resembles that of a type I isotherm. Based on the International Union of Pure and Applied Chemistry (IUPAC) classification, Type I, the mostly microporous structure is crucial to highlight, indicating the materials have a strong affinity between adsorbent and adsorbate (Borhan et al. 2019). Figure 1B presents the mesopore size distribution for FE_7AC and $FE_{22}AC$, and the pore structure consists basically of micropores present 2–3 nm. These results are mainly defined predominantly in micropores together with a small external surface of FE_7AC and $FE_{22}AC$. Similarly, Yu et al. (2019) prepared TACs from tobacco stems by $ZnCl_2$ and TAC1, TAC3, TAC5, and TAC9 display a Type I isotherm as predominated by their micropores. El Nemr et al. (2022) studied to produce SBAC from sugarcane bagasse. They calculated its pore structure by N_2 adsorption isotherms correlated to Type I as microporous.

Surface morphology has an essential role in the activity of the FEB, FE_7AC, and $FE_{22}AC$ by using a scanning electron microscope. These results revealed the pores having the best performance and showed the developed natures of the FE7AC and FE22AC after chemical activation compared to FEB. Figure 2A presents that FEB has no visible pores, although Fig. 2B and C shows irregular pore structures after HCl and KOH activation. Figure 2C shows higher porosity than Fig. 2B due to different preparation, indicating cavities and blanks. The surface area of the FE_7AC and $FE_{22}AC$ differed; however, there was no difference in porosity because structural degradation with HCl has a higher effect than KOH disintegration. There is a comparable difference between FE_7AC and $FE_{22}AC$ during different synthesis forms. The precursors were impregnated by reacting chemicals, both acid and/or base, which occurs ACs with various morphological changes of final materials. Many SEM examinations revealed that ACs have a cavity surface with circularly shaped macropores of multiple sizes. If lignin-containing raw materials are used, ACs have rough characters, recessed and protruding porous (Contescu et al. 2018; Tsai and Jiang 2018; Mistar et al. 2020; Hassan et al. 2020). As reviewed in the literature for ACs obtained from lignocellulosic precursors, Abd-Rabboh et al. (2022) reported the well-developed pores, cavities, and heterogeneous amorphous surface texture on ACs from rice husk and straw wastes. According to Laksaci et al. (2017), ACs were synthesized carbonaceous materials using coffee grounds via KOH, namely ACK9, ACK18, and ACK36, which exhibit their heterogeneous surface and porous nature. Selvaraju and Bakar (2017) benefit from *Artocarpus integer* to develop AFP AC for adsorption applications. The character of AFP AC observed irregular pores-cracks and heterogeneous surfaces. From here, it is possible to know that the porous structure can be highly developed, although generally, they have non-homogeneous surfaces and pores.

Figure 3 displays the FTIR spectra of FEB, FE_7AC, and $FE_{22}AC$ which FEB comprises several functional groups such as the hydroxylic, carboxyl, and carbonyl groups. The broad absorption bands of FE_7AC and $FE_{22}AC$ for the presence of hydroxyl groups were observed at absorption peaks 3287 and 3183 cm^{-1} by stretching vibration of OH bonds (alcohols, phenols, and carboxylic acids). The presence of a wide peak between 2689 and 2704 cm^{-1} may be ascribed to the aliphatic CH stretching in alkyl groups. The bands between 1526 and 1587 cm^{-1} correspond to aromatic ring vibrations the for FE_7AC and $FE_{22}AC$, and the stretching band at 1072 and 1047 cm^{-1} was attributed to the vibration groups of (C–O) and (C–N) in hemicellulose and cellulose. It was also seen that FE_7AC and $FE_{22}AC$ obtained higher intensity adsorption bands compared to virgin

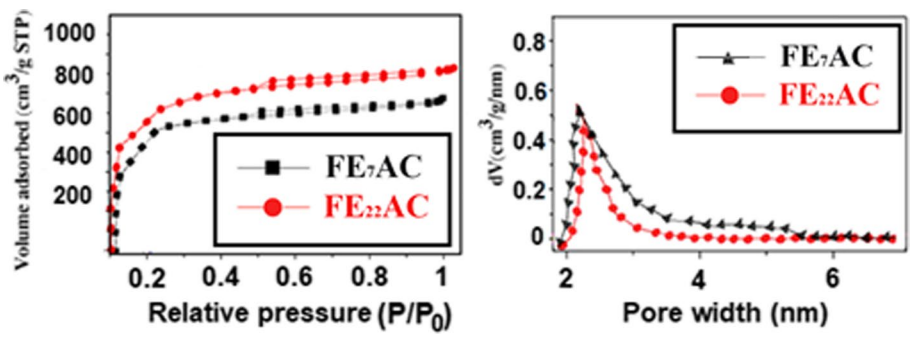

Fig. 1 N_2 adsorption–desorption isotherms at – 196 °C of FE_7AC and $FE_{22}AC$ (**A**) and their pore size distribution (**B**)

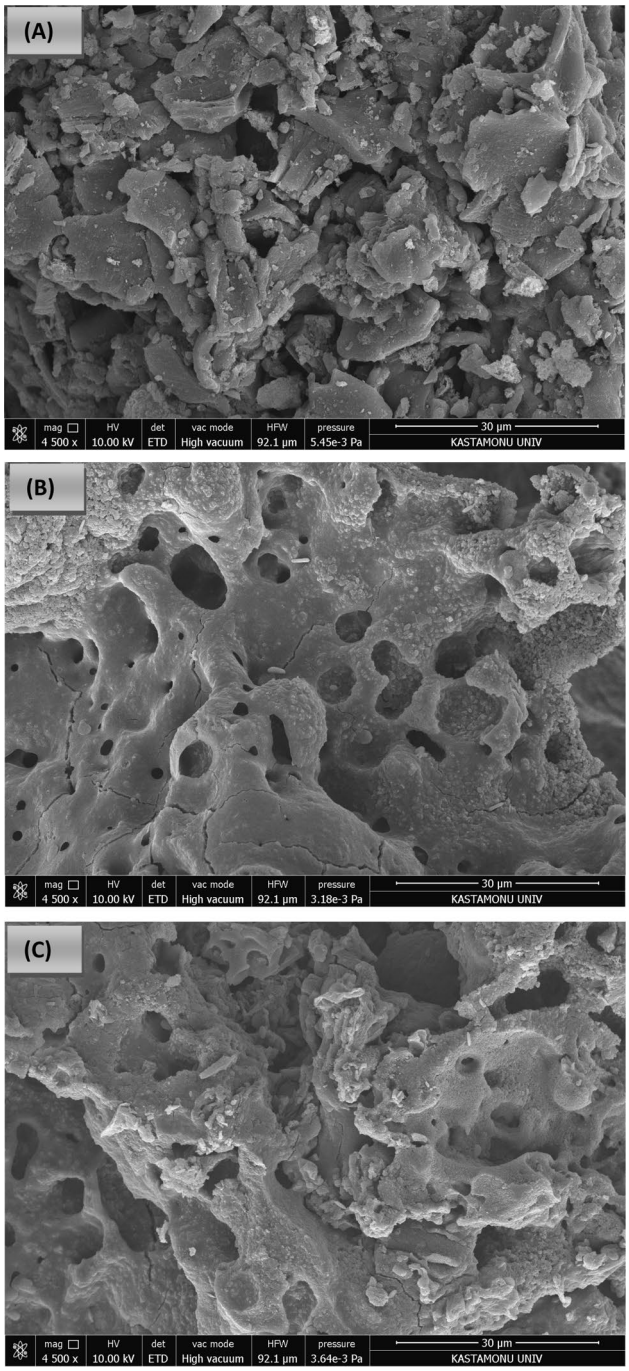

Fig. 2 SEM surface morphologies of FEB (**A**), FE_7AC (**B**), and $FE_{22}AC$ (**C**)

FEB displaying increased amounts of carbon–oxygen and hydroxyl surface groups. The results of these studies are similar to those of other studies in which the formation of surface oxygen-containing functional groups on the adsorbent material which have played an essential role in the formation of some pores in the adsorption capacity by Zhao et al. (2020) and Tran et al. (2021).

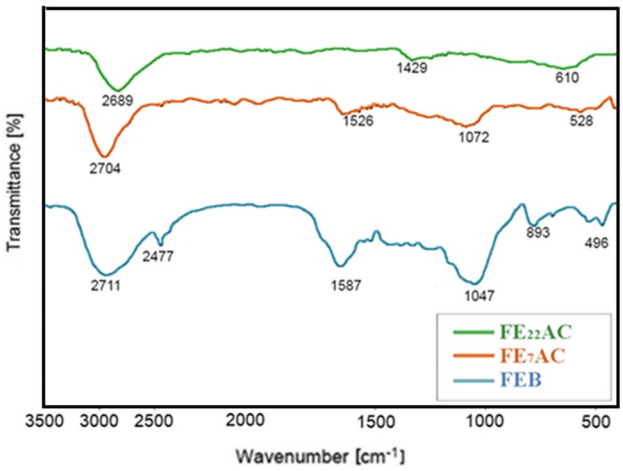

Fig. 3 FT-IR spectra of FEB, FE_7AC, and $FE_{22}AC$

The FEACs were analyzed using Brunauer–Emmet–Teller (BET) analyzer to investigate the surface area, pore volume, and pore size, as shown in Table 3. Notably, the highest surface area, pore volume, and pore size of FE_7AC for HCl and $FE_{22}AC$ for KOH were observed as 676 and 734 m^2/g; 0.39 and 0.48 cm^3/g and 2.53 and 1.97 nm, respectively. This is contributory to the HCl being impregnated on FEB; the pore size, surface area, and pore volume of the FE_7AC decreased compared to $FE_{22}AC$ due to the difference in the action of HCl and KOH.

In several studies, the KOH activation method produced ACs with more microporosity than other chemicals (Wei et al. 2016; Li et al. 2017; Isinkaralar 2022b). For this purpose, Kharrazi et al. (2020) enhanced AC from an elm tree as a lignocellulosic waste sample for batch metal adsorption experiments. They tried to prepare chemical activation with KOH at 800 °C, inferred non-treated AC (465 m^2/g), and thermal tension-treated AC (1085 m^2/g). Samiyammal et al. (2022) used KOH to prepare AC for dye removal from cashew nut shells which obtained the highest surface area of 407.80 m^2/g. Yang et al. (2022) emphasized that the KOH activation ratio of 1:1 (w/w) affects the preparation of AC from a by-product of low-rank coal by microwave method. The methylene blue adsorption was tried to remove using MKBC (their adsorbent name) effectively, and its surface area was reported as 857 m^2/g. The significant difference of KOH activation is more effective than other activating agents, which results in more –OH functional groups on the surface of the ACs. In addition, potassium readily derives its carbon-intercalation compounds, thereby improving the adsorption mechanism of the ACs.

X-ray diffractogram of the fabricated FE_7AC and $FE_{22}AC$ samples has been measured using XPowder of version 2004 graphic tool for powder diffraction in Fig. 4. The diffractograms pattern of FE_7AC and $FE_{22}AC$ was impregnated by

Table 3 Surface areas and pore texture characteristics of FEACs

ACs ID	S_{BET} (m^2/g)	*V*total (cm^3/g)	*V*micro (cm^3/g)	*V*meso (cm^3/g)	*V*micro/*V*total (%)	*V*meso/*V*total (%)	D_p(nm)
FE_1AC	85	0.12	0.08	0.04	66.67	33.33	3.26
FE_2AC	109	0.18	0.11	0.07	61.11	38.89	3.80
FE_3AC	226	0.26	0.19	0.07	73.08	26.92	2.58
FE_4AC	334	0.29	0.21	0.08	72.41	27.59	2.67
FE_5AC	192	0.15	0.09	0.06	60.00	40.00	2.55
FE_6AC	351	0.24	0.14	0.10	58.33	41.67	2.90
FE_7AC	676	0.39	0.25	0.14	64.10	35.90	2.53
FE_8AC	588	0.33	0.23	0.10	69.70	30.30	3.51
FE_9AC	208	0.17	0.11	0.06	64.71	35.29	3.05
$FE_{10}AC$	293	0.29	0.23	0.06	79.31	20.69	2.73
$FE_{11}AC$	547	0.37	0.27	0.10	72.97	27.03	2.59
$FE_{12}AC$	521	0.36	0.25	0.11	69.44	30.56	2.44
$FE_{13}AC$	116	0.18	0.13	0.05	72.22	27.78	3.08
$FE_{14}AC$	238	0.25	0.16	0.09	64.00	36.00	3.42
$FE_{15}AC$	366	0.36	0.26	0.10	72.22	27.78	1.95
$FE_{16}AC$	458	0.33	0.20	0.13	60.61	39.39	2.43
$FE_{17}AC$	139	0.22	0.15	0.07	68.18	31.82	2.25
$FE_{18}AC$	308	0.29	0.22	0.07	75.86	24.14	2.61
$FE_{19}AC$	445	0.38	0.29	0.09	76.32	23.68	2.40
$FE_{20}AC$	543	0.33	0.25	0.08	75.76	24.24	3.48
$FE_{21}AC$	267	0.26	0.18	0.08	69.23	30.77	2.75
$FE_{22}AC$	734	0.48	0.34	0.14	70.83	29.17	1.97
$FE_{23}AC$	630	0.39	0.33	0.06	84.62	15.38	1.35
$FE_{24}AC$	557	0.44	0.32	0.12	72.73	27.27	2.17

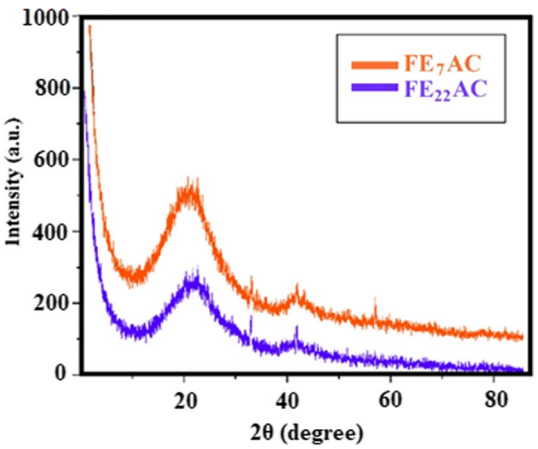

Fig. 4 XRD patterns of FE_7AC and $FE_{22}AC$

HCl and KOH at different activation temperatures and times. The apparent peaks: the first cluster provided 2θ X-ray diffractogram from 5° to 10°, the second one provided peaks at 22.3° and 24.5°, and the third one attained peaks of FE_7AC is detected 34.5 and 57.2°. XRD analysis of $FE_{22}AC$ depicts 32.6° and 41.8°. The above results tell you how high the relative quantity and density of atomic clusters is. It also clearly shows that there are more atoms. The activating of FEB leads to the substantial degradation of lignocellulosic material. The latter accelerates peak intensities of the FE_7AC, and $FE_{22}AC$ has a higher carbon yield than FEB due to higher activation temperature and longer activation time. Mohammed et al. 2020) studied XRD analysis of TPAC from tangerine peel and reported similar results. The broad diffraction peaks between 25.18° and 45.85° confirm the presence of graphite crystallite in TPAC is the expected structure for its adsorption mechanism. Chouikhi et al. (2021) peaks were observed in biochars and ACs, which were attained at diffraction angles (2*θ*) with corresponding planes between 25° and 44°. In many cases, some researchers show similar successfully formed and supported chemical bonds between their biomass during carbonization on the crystallinity of the ACs by Tiegam et al. (2021) and Xue et al. (2022).

The thermal decomposition of FEB, FE_7AC, and $FE_{22}AC$ under an N_2 atmosphere is shown in Fig. 5. In the samples of the three materials, the TGA weight loss curves define three main stages typical for FEB pyrolysis. The first stage corresponds to moisture release, roughly examined at 35–190 °C. The remaining two steps are connected to active and passive pyrolysis; the most significant mass loss characterizes the active stage. Herein, various vapors and gases are released

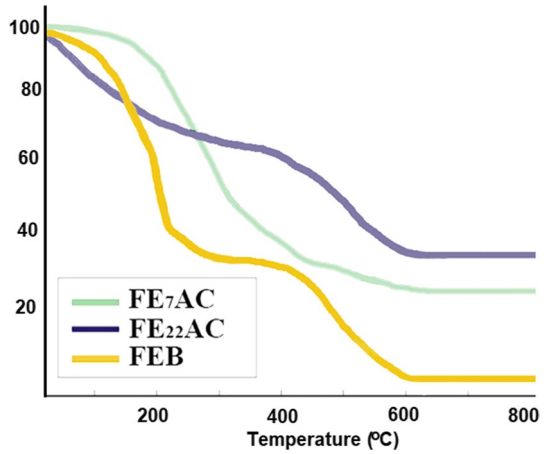

Fig. 5 Thermal stability analysis of FEB, FE_7AC, and $FE_{22}AC$

due to the decomposition processes of hemicelluloses and cellulose, which happen in this stage between 190–440 °C and 450–580 °C, respectively. Shrestha and Rajbhandari (2021) showed weight loss of their raw material, which exhibited significant weight loss at 300–400 °C due to the breakdown of cellulose into components. In addition, the TGA curve revealed that all FE_7AC and $FE_{22}AC$ were thermally stable up to 850 °C. It can be observed that with an increase in the heating rate that the mass losses occur at increasing temperatures. This behavior has been described by (Alghamdi et al. 2019) and (Hossain et al. 2022) can be explained using different arguments. The thermo-gravimetric curves highlighting the mentioned losses of mass can be achieved, suggesting that chemical activation with HCl and KOH resulted in a considerable degree of functional formation on the excellent thermal stability of FE_7AC and $FE_{22}AC$.

Adsorption of benzene vapor

Saturated adsorption capacity

Adsorption studies were carried out at operating temperatures of 20, 25, 30, and 35 °C. The amount of adsorbent used was loaded into the system as 0.5 and 1 g. System operation was started without adsorbent and was monitored until it became stable. Then the different concentration amounts were given to the system; From 5 to 100, the effects of adsorbents were investigated, and although the amount doubled, the adsorbed amount did not double. Based on Fig. 6, the values obtained for FE_7AC and $FE_{22}AC$ at 0.5 and 1 g, up to 100 mg/m^3; (i) 132 and 193 mg/g at 20 °C operating conditions; 151 and 237 mg/g, (ii) 146 and 224 mg/g at

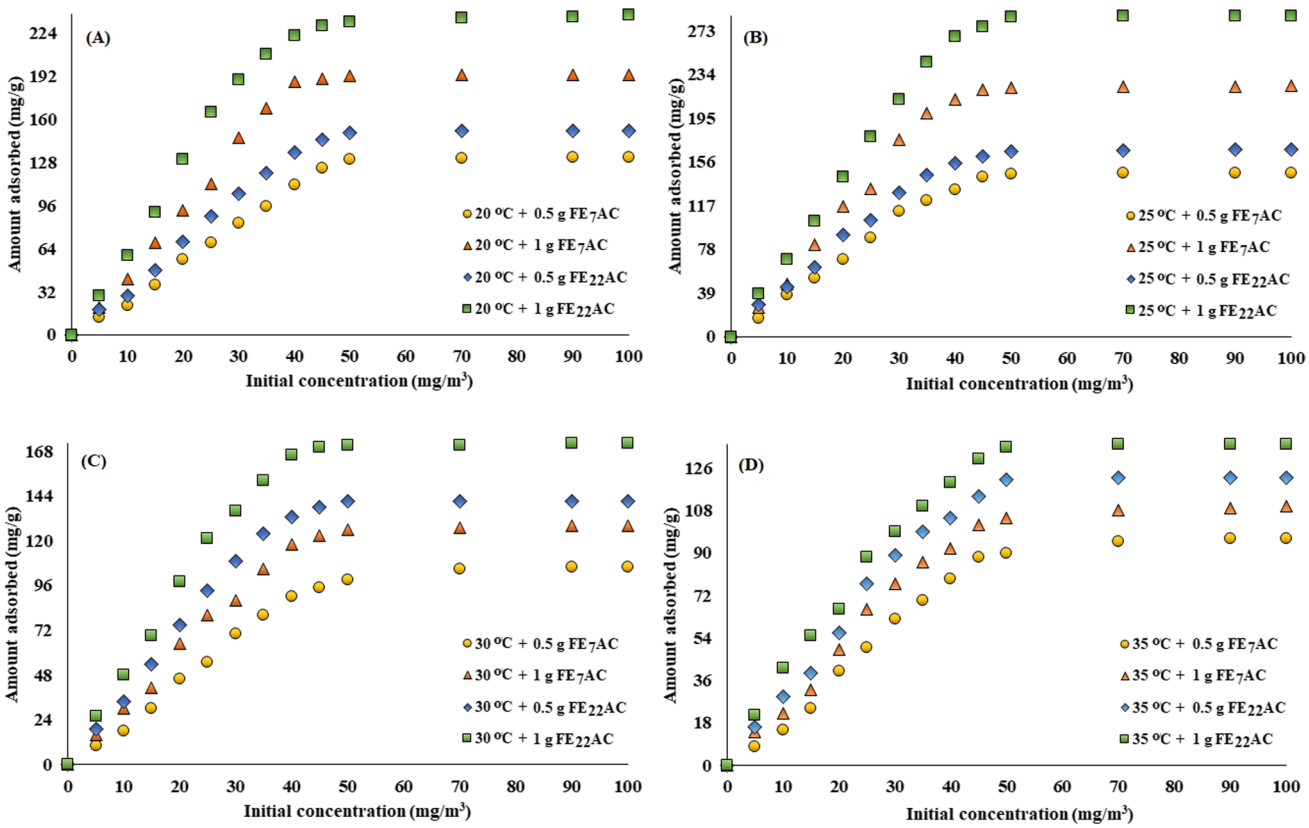

Fig. 6 Steam temperatures (**A**): 20 °C, (**B**): 25°C, (**C**): 30 °C and (**D**): 35 °C for different initial concentrations on the different amounts of FE_7AC and $FE_{22}AC$

25 °C operating conditions; 167 and 286 mg/g, (iii) 106 and 128 mg/g at 30 °C operating conditions; 141 and 172 mg/g, (iv) 96 and 110 mg/g at 35 °C operating conditions; 122 and 136 mg/g. The increase in temperature caused an increase in the adsorption capacity up to 25 °C and then a decrease in the amount of adsorption when it reached 35 °C. The authors indicated that the experiments emphasized positive correlations between benzene molecules and increased initial benzene concentration (Moussavi et al. 2013; Konggidinata et al. 2017; Valencia et al. 2022).

Experimental studies report that the adsorption ability with carbonaceous samples has been affected not only by their prepared methods but also has been impressed, such as existing benzene concentrations by Mataji and Khoshandam 2014; Mohammed et al. 2015 and de Mello et al. 2022. Relatedly, Shi et al. (2022) investigated the gaseous benzene adsorption onto AC7 (S_{BET}: 2669.40 m^2/g) under initial concentrations (1000–5000 ppm) and environmental temperatures (25, 35, and 45 °C). They proved that the driving force of mass transfer was raised due to the growth of the initial concentration. Stähelin et al. (2018) measured the maximum adsorption capacity of benzene in both monocomponent and monocomponent processes. The bicomponent and monocomponent systems were operated with several initial benzenes from 56 to 450 mmol/L and 113 to 450 mmol/L onto ACC from coconut shell. Benzene concentration at higher initial values increases the adsorption capacity. He et al. (2021) utilized PAC-5–850-60 to remove gaseous benzene, which was carried out to explore the maximum diffusion of benzene molecules with the increase in the initial concentration (from 100 to 5000 ppm). The maximum adsorption capacity for 100, 1000, and 5000 ppm was calculated at 122.19, 437.11, and 819.77 mg/g for PAC-5–850-60.

Adsorption equilibrium time

The adsorbent amount was fixed at 0.5 and 1 g, and the adsorption capacities up to 200 min were compared by increasing the system's temperature. Plausibly, the results were compared for 0.5 and 1 g FE_7AC and $FE_{22}AC$ was injected with 100 mg/m^3 benzene as an initial concentration. Respectively, when the values obtained for FE_7AC and $FE_{22}AC$ at 20, 25, 30, and 35 °C were compared, as shown in Fig. 7, they adsorbed more than 65% in the first 20 min. It was observed that the limit values were reached in adsorption capacities between 20 and 50 min. However, the adsorbents were expected to reach equilibrium conditions, and adsorption stopped at 200 min. This evidence suggests

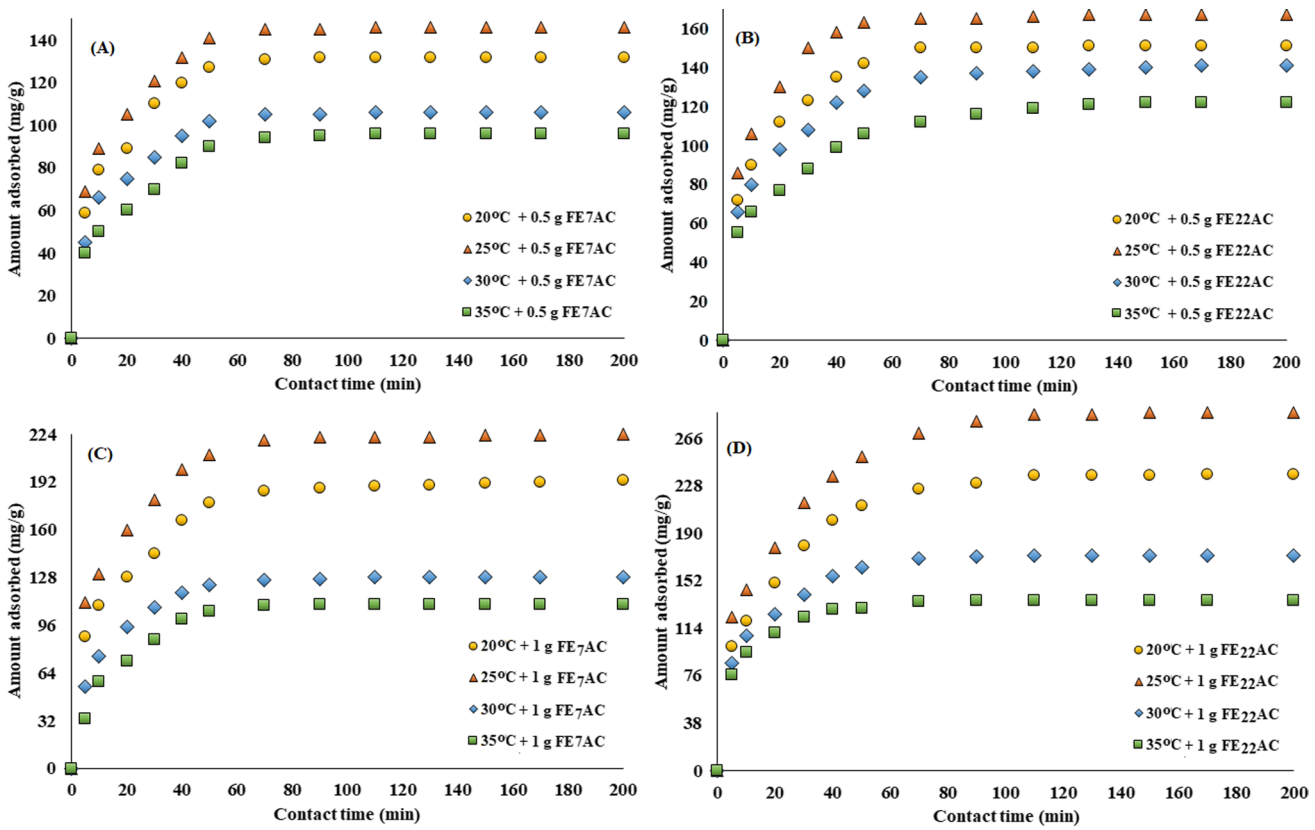

Fig. 7 Comparison of residence time curves on the different amounts (**A**): 0.5 g FE_7AC, (**B**): 0.5 g $FE_{22}AC$, (**C**): 1 g of FE_7AC and (**D**): 1 g of $FE_{22}AC$

a link between dramatically decreasing benzene adsorption amount and rising temperature effects on a potential loss of adsorptive benzene molecules due to their behaviors becoming more active at ≥ 25 °C. It is indispensable to be aware of the increasing temperature for benzene adsorption; thus, research results have been consistent with our findings. In Li et al. (2020a, b) research, the benzene adsorption rate investigated the filling pore process on carbon adsorbents (AC-1, AC-2, AC-3, and AC-4) under different temperatures (0, 15, 30, and 45 °C). Their results indicate that the adsorption amount of the AC-1 and AC-2 changed little with temperature; however, the adsorption values of the AC-3 decreased until 30 °C. The AC-3 obtained more excellent adsorption due to its larger micropores than others. Chen et al. (2023) systematically employed dynamic benzene adsorption on hollow carbon spheres (HCS-11 S_{BET}: 2531.29 m^2/g and S_{Micro}: 3.527 m^2/g) and commercial coal-based AC (CBAC S_{BET}: 1109 0.44 m^2/g and S_{Micro}: 0.459 m^2/g) at 20, 30, and 40 °C. The saturated adsorption capacities compared between HCS-11 and CBAC at 20, 30, and 40 °C were 21.363–5.889, 20.389–5.716, and 19.981–5.617 mmol/g. The results appeared the adsorption capacity slowed down with increased temperature. Also, the CBAC showed a relatively minor adsorption amount than HCS-11 due to a smaller proportion of micropores. Several researchers indicate positive correlations between benzene rings and the increase in temperature (Saleh and Danmaliki 2016; Deng et al. 2021; Jareteg et al. 2021).

Adsorption technology has been widely used to prevent the problems caused by exposure to benzene gas at different concentrations. In addition, some literature has reported that the production and modification of various adsorbents increased, accelerating the adsorption efficiency (Martínez de Yuso et al. 2013; Dizbay-Onat et al. 2018; Gayathiri et al. 2022). While the increases were realized, the production phase was left behind regarding environmentalist, sustainability, and cost–benefit. However, the production steps of the lignin-containing adsorbent used in this study are quite reasonable, low-budget, easy to apply, high in surface area and pore volume, and include environmentally friendly approaches. Moreover, a large number of initiatives have produced adsorbents with cheap, renewable (Saadi et al. 2022) and abundant biomass (İlbay et al. 2017), but they have removed pollutants in liquid media, not in gaseous media (Karimnezhad et al. 2014; Anand et al. 2021). Although the research is limited to the gaseous environment, some people have made different VOC removals (Khan et al. 2019; Ma et al. 2021). The effective point in these studies is the simultaneous multiple degassing or a single type of degassing. An example of these efforts is the effectiveness of adsorbents used in multiple degassing is much less than those used in single degassing (Osuchowski et al. 2019). In systems working as multi-component, different molecular structures entering the pores of the adsorbent and their filling of the pores are in a dispersed, unsystematic form without being homogeneous; in a system, which works as a single component, it is noteworthy that the molecules filling the pores are homogeneous, more systematic and stable (Lee et al. 2019). In particular, the filling of the pores of several adsorbents occurs differently from each other (Feng et al. 2023). The homogeneous structure of the pores is seen to be less in number, although it is more systematic while taking in the molecules. However, studies have shown that the heterogeneous structure obtained after activating lignin-containing structures includes benzene molecules (Saha et al. 2018). Based on these studies, general judgments can be reached by comparison measurements under different conditions, as differences arise in terms of characteristics such as reactor type (discrete, continuous, etc.) (Azhagapillai et al. 2021), adsorbent structure and amount (Kim et al. 2021b), multi- or single component (Ouzzine et al. 2019), the molecular structure of the gas to be removed, ambient temperature-humidity (Oh et al. 2019), and contact time (Qiao et al. 2021).

Conclusion

Developing the surface area on the gaseous benzene removal efficiency is a vital recoverer to indoor air pollution. Indoor air quality must be unquestionably good in areas that cannot be ventilated, in public transportation, indoors, shopping malls, vehicle and air conditioner filters, health centers, and schools. The production of $FE_{22}AC$ with high adsorption capacity using an economical and straightforward technique can still be a great subject to inspect biomass transformation into carbonaceous materials by chemical activation. The adsorbing ability of the produced activated carbon up to 200 min was examined, and the results were exhibited on its adsorptive potential. A microporous $FE_{22}AC$ having a high surface area and total pore volume (676 m^2/g and 0.39 cm^3/g) resulted from KOH impregnation under 1:3 (w/w) carbonized at 700 °C for 2 h of activation time. The deposited directly onto the $FE_{22}AC$ from the gaseous environment resulted in its highest potential of 286 mg/g at the ambient temperature of 25 °C at an initial benzene concentration of 100 mg/m^3 and for 200 min. Another powerful adsorbent is FE_7AC which has a lower adsorption capacity than $FE_{22}AC$ because of its physical and chemical characteristics. This would specifically help to reveal economic and eco-friendly gas benzene capture mechanism was found desirable for good biosorption potential and reuse of recycled materials.

Author contribution statement This study was entirely prepared by KI.

Funding Not applicable.

Availability of data and materials The data that support the findings of this study are available from the corresponding author, upon reasonable request.

Declarations

Conflict of interest The author declares no competing interests.

Ethical approval Not applicable.

References

Abd-Rabboh HS, Fawy KF, Hamdy MS, Elbehairi SI, Shati AA, Alfaifi MY, Ibrahium HA, Alamri S, Awwad NS (2022) Valorization of rice husk and straw agriculture wastes of Eastern Saudi Arabia: production of bio-based silica, lignocellulose, and activated carbon. Materials 15(11):3746. https://doi.org/10.3390/ma15113746

Alghamdi AA, Al-Odayni AB, Saeed WS, Al-Kahtani A, Alharthi FA, Aouak T (2019) Efficient adsorption of lead (II) from aqueous phase solutions using polypyrrole-based activated carbon. Materials 12(12):2020. https://doi.org/10.3390/ma12122020

Anand B, Szulejko JE, Kim KH, Younis SA (2021) Proof of concept for CUK family metal-organic frameworks as environmentally-friendly adsorbents for benzene vapor. Environ Poll 285:117491. https://doi.org/10.1016/j.envpol.2021.117491

Arminda M, Josúe C, Cristina D, Fabiana S, Yolanda M (2021) Use of activated carbons for detoxification of a lignocellulosic hydrolysate: Statistical optimisation. J Environ Manag 296:113320. https://doi.org/10.1016/j.jenvman.2021.113320

ASTM D1102–84, (2013). Standard test method for ash in wood ASTM international, West Conshohocken: Philadelphia, PA

ASTM E871–82 (2019) Standard test method for moisture analysis of particulate wood fuels ASTM international, West Conshohocken: Philadelphia, PA

ASTM E872–82 (2019) Standard test method for volatile matter in the analysis of particulate wood fuels ASTM international, West Conshohocken: Philadelphia, PA

ASTM (2011) Standard test method for volatile matter in the analysis sample of coal and coke. In: D3175–11

Azhagapillai P, Al Shoaibi A, Chandrasekar S (2021) Surface functionalization methodologies on activated carbons and their benzene adsorption. Carbon Lett 31:419–426. https://doi.org/10.1007/s42823-020-00170-w

Borhan A, Yusup S, Lim JW, Show PL (2019) Characterization and modelling studies of activated carbon produced from rubber-seed shell using KOH for CO_2 adsorption. Processes 7(11):855. https://doi.org/10.3390/pr7110855

Boundzanga HM, Cagnon B, Roulet M, de Persis S, Vautrin-Ul C, Bonnamy S (2020) Contributions of hemicellulose, cellulose, and lignin to the mass and the porous characteristics of activated carbons produced from biomass residues by phosphoric acid activation. Biomass Convers Biorefinery. https://doi.org/10.1007/s13399-020-00816-9

Brdarić D, Kovač-Andrić E, Šapina M, Kramarić K, Lutz N, Perković T, Egorov A (2019) Indoor air pollution with benzene, formaldehyde, and nitrogen dioxide in schools in Osijek, Croatia. Air Qual Atmos Health 12:963–968. https://doi.org/10.1007/s11869-019-00715-7

Chaiklieng S, Suggaravetsiri P, Autrup H (2019) Risk assessment on benzene exposure among gasoline station workers. Int J Environ Res Public Health 16(14):2545. https://doi.org/10.3390/ijerph16142545

Chen G, Yang X, Ma Y, Ruan C, Chen Q, Jin X, Sun J, He S (2023) Structurally controllable hollow carbon spheres for gaseous benzene adsorption. J Environ Chem Eng 11(1):109182. https://doi.org/10.1016/j.jece.2022.109182

Chouikhi N, Cecilia JA, Vilarrasa-García E, Serrano-Cantador L, Besghaier S, Chlendi M, Bagane M, Castellón ER (2021) Valorization of agricultural waste as a carbon materials for selective separation and storage of CO_2, H_2 and N_2. Biomass Bioenergy 155:106297. https://doi.org/10.1016/j.biombioe.2021.106297

Contescu CI, Adhikari SP, Gallego NC, Evans ND, Biss BE (2018) Activated carbons derived from high-temperature pyrolysis of lignocellulosic biomass. C 4(3):51. https://doi.org/10.3390/c4030051

de Mello R, Motheo AJ, Saez C, Rodrigo MA (2022) Combination of granular activated carbon adsorption and electrochemical oxidation processes in methanol medium for benzene removal. Electrochim Acta. https://doi.org/10.1016/j.electacta.2022.140681

Deng H, Kang S, Ma J, Zhang C, He H (2018) Silver incorporated into cryptomelane-type manganese oxide boosts the catalytic oxidation of benzene. Appl Catal B 239:214–222. https://doi.org/10.1016/j.apcatb.2018.08.006

Deng Z, Deng Q, Wang L, Xiang P, Lin J, Murugadoss V, Song G (2021) Modifying coconut shell activated carbon for improved purification of benzene from volatile organic waste gas. Adv Compos Hybrid Mater 4(3):751–760. https://doi.org/10.1007/s42114-021-00273-6

Department of Environmental health (2017) Department of Environmental health Environmental Health in Israel

Dizbay-Onat M, Floyd E, Vaidya UK, Lungu CT (2018) Applicability of industrial sisal fiber waste derived activated carbon for the adsorption of volatile organic compounds (VOCs). Fibers Polym 19:805–811. https://doi.org/10.1007/s12221-018-7866-z

El Nemr A, Aboughaly RM, El Sikaily A, Masoud MS, Ramadan MS, Ragab S (2022) Microporous-activated carbons of type I adsorption isotherm derived from sugarcane bagasse impregnated with zinc chloride. Carbon Lett 32(1):229–249. https://doi.org/10.1007/s42823-021-00270-1

Environ (2014) Environ project environmental and social standards-yamal LNG project

Feng C, Deng Y, Jiaqiang E, Han D, Tan Y (2023) Effect analysis on hydrocarbon adsorption enhancement of ZSM-5 zeolite modified by transition metal ions in cold start of gasoline engine. Energy 267:126554. https://doi.org/10.1016/j.energy.2022.126554

Fetisov V, Gonopolsky AM, Davardoost H, Ghanbari AR, Mohammadi AH (2023) Regulation and impact of VOC and CO_2 emissions on low-carbon energy systems resilient to climate change: a case study on an environmental issue in the oil and gas industry. Energy Sci Eng 11(4):1516–1535

Flanagan J, Meyer M, Pasamar MA, Ibarra A, Roller M, iGenoher NA, Leiva S, Gomez-García F, Alcaraz M, Martínez-Carrasco A, Vicente V (2013) Safety evaluation and nutritional composition of a Fraxinus excelsior seed extract, FraxiPure™. Food Chem Toxicol 53:10–17. https://doi.org/10.1016/j.fct.2012.11.030

Franco DS, Georgin J, Netto MS, Allasia D, Oliveira ML, Foletto EL, Dotto GL (2021) Highly effective adsorption of synthetic phenol effluent by a novel activated carbon prepared from fruit wastes of the Ceiba speciosa forest species. J Environ Chem Eng 9(5):105927

Gao Y, Yue Q, Gao B, Li A (2020) Insight into activated carbon from different kinds of chemical activating agents: a review. Sci Total Environ 746:141094. https://doi.org/10.1016/j.scitotenv.2020.141094

Gayathiri M, Pulingam T, Lee KT, Sudesh K (2022) Activated carbon from biomass waste precursors: factors affecting production and

adsorption mechanism. Chemosphere. https://doi.org/10.1016/j.chemosphere.2022.133764
González-García P (2018) Activated carbon from lignocellulosics precursors: a review of the synthesis methods, characterization techniques and applications. Renew Sustain Energy Rev 82:1393–1414. https://doi.org/10.1016/j.rser.2017.04.117
Hassan MF, Sabri MA, Fazal H, Hafeez A, Shezad N, Hussain M (2020) Recent trends in activated carbon fibers production from various precursors and applications—a comparative review. J Anal Appl Pyrolysis 145:104715. https://doi.org/10.1016/j.jaap.2019.104715
He S, Shi G, Xiao H, Sun G, Shi Y, Chen G, Dai H, Yuan B, Chen X, Yang X (2021) Self S-doping activated carbon derived from lignin-based pitch for removal of gaseous benzene. Chem Eng J 410:128286. https://doi.org/10.1016/j.cej.2020.128286
Heidarinejad Z, Dehghani MH, Heidari M, Javedan G, Ali I, Sillanpää M (2020) Methods for preparation and activation of activated carbon: a review. Environ Chem Lett 18:393–415. https://doi.org/10.1007/s10311-019-00955-0
Hossain N, Nizamuddin S, Selvakannan P, Griffin G, Madapusi S, Shah K (2022) The effect of KOH activation and Ag nanoparticle incorporation on rice husk-based porous materials for wastewater treatment. Chemosphere 291:132760. https://doi.org/10.1016/j.chemosphere.2021.132760
İlbay Z, Haşimoğlu A, Özdemir OK, Ateş F, Şahin S (2017) Highly efficient recovery of biophenols onto graphene oxide nanosheets: valorisation of a biomass. J Mol Liq 246:208–214. https://doi.org/10.1016/j.molliq.2017.09.046
Isinkaralar K (2022a) High-efficiency removal of benzene vapor using activated carbon from *Althaea officinalis* L. biomass as a lignocellulosic precursor. Environ Sci Poll Res 29(44):66728–66740. https://doi.org/10.1007/s11356-022-20579-2
Isinkaralar K (2022b) Theoretical removal study of gas BTEX onto activated carbon produced from *Digitalis purpurea* L. biomass. Biomass Convers Biorefinery 12(9):4171–4181. https://doi.org/10.1007/s13399-022-02558-2
Isinkaralar K (2023a) A study on the gaseous benzene removal based on adsorption onto the cost-effective and environmentally friendly adsorbent. Molecules 28(8):3453. https://doi.org/10.3390/molecules28083453
Isinkaralar K (2023b) Experimental evaluation of benzene adsorption in the gas phase using activated carbon from waste biomass. Biomass Convers Biorefinery. https://doi.org/10.1007/s13399-023-03979-3
Isinkaralar O (2023c) Bioclimatic comfort in urban planning and modeling spatial change during 2020–2100 according to climate change scenarios in Kocaeli Türkiye. Int J Environ Sci Technol 20(7):7775–7786. https://doi.org/10.1007/s13762-023-04992-9
Isinkaralar K, Turkyilmaz A (2022) Simultaneous adsorption of selected VOCs in the gas environment by low-cost adsorbent from *Ricinus communis*. Carbon Lett 32(7):1781–1789. https://doi.org/10.1007/s42823-022-00399-7
Isinkaralar O, Varol C (2023) A cellular automata-based approach for spatio-temporal modeling of the city center as a complex system: the case of Kastamonu, Türkiye. Cities 132:104073. https://doi.org/10.1016/j.cities.2022.104073
Isinkaralar O, Varol C, Yilmaz D (2022) Digital mapping and predicting the urban FEowth: intefeating scenarios into cellular automata—Markov chain modeling. Appl Geom 14(4):695–705. https://doi.org/10.1007/s12518-022-00464-w
Jang J, Son M, Chung S, Kim K, Cho C, Lee BH, Ham MH (2015) Low-temperature-grown continuous graphene films from benzene by chemical vapor deposition at ambient pressure. Sci Rep 5(1):17955. https://doi.org/10.1038/srep17955
Jareteg A, Maggiolo D, Thunman H, Sasic S, Ström H (2021) Investigation of steam regeneration strategies for industrial-scale temperature-swing adsorption of benzene on activated carbon. Chem Eng Process-Process Intensif 167:108546. https://doi.org/10.1016/j.cep.2021.108546
Karimnezhad L, Haghighi M, Fatehifar E (2014) Adsorption of benzene and toluene from waste gas using activated carbon activated by $ZnCl_2$. Front Environ Sci Eng 8(6):835–844. https://doi.org/10.1007/s11783-014-0695-4
Khan A, Szulejko JE, Kim KH, Sammadar P, Lee SS, Yang X, Ok YS (2019) A comparison of figure of merit (FOM) for various materials in adsorptive removal of benzene under ambient temperature and pressure. Environ Res 168:96–108. https://doi.org/10.1016/j.envres.2018.09.019
Kharrazi SM, Mirghaffari N, Dastgerdi MM, Soleimani M (2020) A novel post-modification of powdered activated carbon prepared from lignocellulosic waste through thermal tension treatment to enhance the porosity and heavy metals adsorption. Powder Technol 366:358–368. https://doi.org/10.1016/j.powtec.2020.01.065
Kim NS, Oh M, Kim K, Jo C (2021a) 3D graphene-like zeolite-templated carbon with hierarchical structures as a high-performance adsorbent for volatile organic compounds. Chem Eng J 409:128076. https://doi.org/10.1016/j.cej.2020.128076
Kim WK, Younis SA, Kim KH (2021b) A strategy for the enhancement of trapping efficiency of gaseous benzene on activated carbon (AC) through modification of their surface functionalities. Environ Pollut 270:116239. https://doi.org/10.1016/j.envpol.2020.116239
Konggidinata MI, Chao B, Lian Q, Subramaniam R, Zappi M, Gang DD (2017) Equilibrium, kinetic and thermodynamic studies for adsorption of BTEX onto ordered mesoporous carbon (OMC). J Hazard Mater 336:249–259. https://doi.org/10.1016/j.jhazmat.2017.04.073
Kwiatkowski M, Broniek E (2017) An analysis of the porous structure of activated carbons obtained from hazelnut shells by various physical and chemical methods of activation. Colloids Surf A 529:443–453. https://doi.org/10.1016/j.colsurfa.2017.06.028
Laksaci H, Khelifi A, Trari M, Addoun A (2017) Synthesis and characterization of microporous activated carbon from coffee grounds using potassium hydroxides. J Clean Prod 147:254–262. https://doi.org/10.1016/j.jclepro.2017.01.102
Largitte L, Brudey T, Tant T, Dumesnil PC, Lodewyckx P (2016) Comparison of the adsorption of lead by activated carbons from three lignocellulosic precursors. Microporous Mesoporous Mater 219:265–275. https://doi.org/10.1016/j.micromeso.2015.07.005
Lee KLK, McGuire BA, McCarthy MC (2019) Gas-phase synthetic pathways to benzene and benzonitrile: a combined microwave and thermochemical investigation. Phys Chem Chem Phys 21(6):2946–2956. https://doi.org/10.1039/C8CP06070C
Li S, Han K, Li J et al (2017) Preparation and characterization of super activated carbon produced from gulfweed by KOH activation. Microporous Mesoporous Mater 243:291–300. https://doi.org/10.1016/j.micromeso.2017.02.052
Li S, Song K, Zhao D, Rugarabamu JR, Diao R, Gu Y (2020a) Molecular simulation of benzene adsorption on different activated carbon under different temperatures. Microporous Mesoporous Mater 302:110220. https://doi.org/10.1016/j.micromeso.2020.110220
Li X, Zhang L, Yang Z, He Z, Wang P, Yan Y, Ran J (2020b) Hydrophobic modified activated carbon using PDMS for the adsorption of VOCs in humid condition. Sep Purif Technol 239:116517. https://doi.org/10.1016/j.seppur.2020.116517
Liu Y, Zhou H, Cao R, Liu X, Zhang P, Zhan J, Liu L (2019) Facile and green synthetic strategy of birnessite-type MnO_2 with high efficiency for airborne benzene removal at low temperatures. Appl Catal B 245:569–582. https://doi.org/10.1016/j.apcatb.2019.01.023

Liu C, Huang X, Li J (2020) Outdoor benzene highly impacts indoor concentrations globally. Sci Total Environ 720:137640. https://doi.org/10.1016/j.scitotenv.2020.137640

Long C, Li Y, Yu W, Li A (2012) Removal of benzene and methyl ethyl ketone vapor: comparison of hypercrosslinked polymeric adsorbent with activated carbon. J Hazard Mater 203:251–256. https://doi.org/10.1016/j.jhazmat.2011.12.010

Luo T, Wang Z, Wei X, Huang X, Bai S, Chen J (2022) Surface enrichment promotes the decomposition of benzene from air. Catal Sci Technol 12(7):2340–2345. https://doi.org/10.1039/D1CY02296B

Ma X, Ding C, Li D, Wu M, Yu Y (2018) A facile approach to prepare biomass-derived activated carbon hollow fibers from wood waste as high-performance supercapacitor electrodes. Cellulose 25:4743–4755. https://doi.org/10.1007/s10570-018-1903-3

Ma X, Yang L, Wu H (2021) Removal of volatile organic compounds from the coal-fired flue gas by adsorption on activated carbon. J Clean Prod 302:126925. https://doi.org/10.1016/j.jclepro.2021.126925

Martínez de Yuso A, Izquierdo MT, Rubio B, Carrott PJM (2013) Adsorption of toluene and toluene–water vapor mixture on almond shell based activated carbons. Adsorption 19:1137–1148. https://doi.org/10.1007/s10450-013-9540-5

Mataji M, Khoshandam B (2014) Benzene adsorption on activated carbon from walnut shell. Chem Eng Commun 201(10):1294–1313. https://doi.org/10.1080/00986445.2013.808996

Mehralipour J, Jafari AJ, Gholami M, Esrafili A, Kermani M (2022) Synthesis of BiOI@ NH2-MIL125 (Ti)/Zeolite as a novel MOF and advanced hybrid oxidation process application in benzene removal from polluted air stream. J Environ Health Sci Eng. https://doi.org/10.1007/s40201-022-00837-8

Miller D, Armstrong K, Styring P (2022) Assessing methods for the production of renewable benzene. Sustain Prod Consum 32:184–197. https://doi.org/10.1016/j.spc.2022.04.019

Ministry for the Environment (2010) Ministry for the environment clean air conservation act

Mistar EM, Alfatah T, Supardan MD (2020) Synthesis and characterization of activated carbon from *Bambusa vulgaris* striata using two-step KOH activation. J Market Res 9(3):6278–6286. https://doi.org/10.1016/j.jmrt.2020.03.041

Mohammad SG, Ahmed SM, Amr AEGE, Kamel AH (2020) Porous activated carbon from lignocellulosic agricultural waste for the removal of acetampirid pesticide from aqueous solutions. Molecules 25(10):2339. https://doi.org/10.3390/molecules25102339

Mohammed J, Nasri NS, Zaini MAA, Hamza UD, Ani FN (2015) Adsorption of benzene and toluene onto KOH activated coconut shell based carbon treated with NH_3. Int Biodeterior Biodegrad 102:245–255. https://doi.org/10.1016/j.ibiod.2015.02.012

Moussavi G, Rashidi R, Khavanin A (2013) The efficacy of GAC/MgO composite for destructive adsorption of benzene from waste air stream. Chem Eng J 228:741–747. https://doi.org/10.1016/j.cej.2013.05.032

Nayek S, Padhy PK (2020) Personal exposure to VOCs (BTX) and women health risk assessment in rural kitchen from solid biofuel burning during cooking in West Bengal, India. Chemosphere 244:125447. https://doi.org/10.1016/j.chemosphere.2019.125447

Oh JY, You YW, Park J, Hong JS, Heo I, Lee CH, Suh JK (2019) Adsorption characteristics of benzene on resin-based activated carbon under humid conditions. J Ind Eng Chem 71:242–249

Osuchowski Ł, Szczęśniak B, Choma J, Jaroniec M (2019) High benzene adsorption capacity of micro-mesoporous carbon spheres prepared from XAD-4 resin beads with pores protected effectively by silica. J Mater Sci 54(22):13892–13900. https://doi.org/10.1007/s10853-019-03869-y

Ouzzine M, Romero-Anaya AJ, Lillo-Rodenas MA, Linares-Solano A (2019) Spherical activated carbons for the adsorption of a real multicomponent VOC mixture. Carbon 148:214–223. https://doi.org/10.1016/j.carbon.2019.03.075

Padilla O, Gallego J, Santamaría A (2018) Using benzene as growth precursor for the carbon nanostructure synthesis in an inverse diffusion flame reactor. Diam Relat Mater 86:128–138. https://doi.org/10.1016/j.diamond.2018.04.024

Pal VK, Lee S, Naidu M, Lee C, Kannan K (2022) Occurrence of and dermal exposure to benzene, toluene and styrene found in hand sanitizers from the United States. Environ Int 167:107449. https://doi.org/10.1016/j.envint.2022.107449

Pui WK, Yusoff R, Aroua MK (2019) A review on activated carbon adsorption for volatile organic compounds (VOCs). Rev Chem Eng 35(5):649–668. https://doi.org/10.1515/revce-2017-0057

Qiao Y, Lv N, Li D, Li H, Xue X, Jiang W, Xu Z, Che G (2021) Construction of MOF-shell porous materials and performance studies in the selective adsorption and separation of benzene pollutants. Dalton Trans 50(26):9076–9087. https://doi.org/10.1039/D1DT01205C

Quesada HB, de Araújo TP, Vareschini DT, de Barros MASD, Gomes RG, Bergamasco R (2020) Chitosan, alginate and other macromolecules as activated carbon immobilizing agents: a review on composite adsorbents for the removal of water contaminants. Int J Biol Macromol 164:2535–2549. https://doi.org/10.1016/j.ijbiomac.2020.08.118

Rene ER, Kar S, Krishnan J, Pakshirajan K, López ME, Murthy DVS, Swaminathan T (2015) Start-up, performance and optimization of a compost biofilter treating gas-phase mixture of benzene and toluene. Biores Technol 190:529–535. https://doi.org/10.1016/j.biortech.2015.03.049

Saadi W, Rodríguez-Sánchez S, Ruiz B, Najar-Souissi S, Ouederni A, Fuente E (2022) From pomegranate peels waste to one-step alkaline carbonate activated carbons. Prospect as sustainable adsorbent for the renewable energy production. J Environ Chem Eng 10(1):107010. https://doi.org/10.1016/j.jece.2021.107010

Saha D, Mirando N, Levchenko A (2018) Liquid and vapor phase adsorption of BTX in lignin derived activated carbon: equilibrium and kinetics study. J Clean Prod 182:372–378. https://doi.org/10.1016/j.jclepro.2018.02.076

Sakizadeh M (2019) Spatiotemporal variations and characterization of the chronic cancer risk associated with benzene exposure. Ecotoxicol Environ Saf 182:109387. https://doi.org/10.1016/j.ecoenv.2019.109387

Saleem F, Zhang K, Harvey AP (2019) Decomposition of benzene as a tar analogue in CO_2 and H_2 carrier gases, using a non-thermal plasma. Chem Eng J 360:714–720. https://doi.org/10.1016/j.cej.2018.11.195

Saleh TA, Danmaliki GI (2016) Influence of acidic and basic treatments of activated carbon derived from waste rubber tires on adsorptive desulfurization of thiophenes. J Taiwan Inst Chem Eng 60:460–468. https://doi.org/10.1016/j.jtice.2015.11.008

Samiyammal P, Kokila A, Pragasan LA et al (2022) Adsorption of brilliant green dye onto activated carbon prepared from cashew nut shell by KOH activation: studies on equilibrium isotherm. Environ Res 212:113497. https://doi.org/10.1016/j.envres.2022.113497

Sekar A, Varghese GK, Varma MR (2019) Analysis of benzene air quality standards, monitoring methods and concentrations in indoor and outdoor environment. Heliyon 5(11):e02918. https://doi.org/10.1016/j.heliyon.2019.e02918

Selvaraju G, Bakar NKA (2017) Production of a new industrially viable green-activated carbon from Artocarpus integer fruit processing waste and evaluation of its chemical, morphological and adsorption properties. J Clean Prod 141:989–999. https://doi.org/10.1016/j.jclepro.2016.09.056

Shi G, He S, Chen G, Ruan C, Ma Y, Chen Q, Jin X, Liu X, He C, Du C, Dai H, Yang X (2022) Crayfish shell-based micro-mesoporous

activated carbon: Insight into preparation and gaseous benzene adsorption mechanism. Chem Eng J 428:131148. https://doi.org/10.1016/j.cej.2021.131148

Shrestha D, Rajbhandari A (2021) The effects of different activating agents on the physical and electrochemical properties of activated carbon electrodes fabricated from wood-dust of Shorea robusta. Heliyon 7(9):e07917. https://doi.org/10.1016/j.heliyon.2021.e07917

Spatari G, Allegra A, Carrieri M, Pioggia G, Gangemi S (2021) Epigenetic effects of benzene in hematologic neoplasms: the altered gene expression. Cancers 13(10):2392. https://doi.org/10.3390/cancers13102392

Stähelin PM, Valério A, Ulson SMDAG, da Silva A, Valle JAB, de Souza AAU (2018) Benzene and toluene removal from synthetic automotive gasoline by mono and bicomponent adsorption process. Fuel 231:45–52. https://doi.org/10.1016/j.fuel.2018.04.169

Szulejko JE, Kim KH, Parise J (2019) Seeking the most powerful and practical real-world sorbents for gaseous benzene as a representative volatile organic compound based on performance metrics. Sep Purif Technol 212:980–985. https://doi.org/10.1016/j.seppur.2018.11.001

Tiegam RFT, Tchuifon DRT, Santagata R, Nanssou PAK, Anagho SG, Ionel I, Ulgiati S (2021) Production of activated carbon from cocoa pods: Investigating benefits and environmental impacts through analytical chemistry techniques and life cycle assessment. J Clean Prod 288:125464. https://doi.org/10.1016/j.jclepro.2020.125464

Tran TH, Le HH, Pham TH, Nguyen DT, La DD, Chang SW, Lee SM, Chung WJ, Nguyen DD (2021) Comparative study on methylene blue adsorption behavior of coffee husk-derived activated carbon materials prepared using hydrothermal and soaking methods. J Environ Chem Eng 9(4):105362. https://doi.org/10.1016/j.jece.2021.105362

Tsai WT, Jiang TJ (2018) Mesoporous activated carbon produced from coconut shell using a single-step physical activation process. Biomass Convers Biorefinery 8:711–718. https://doi.org/10.1007/s13399-018-0322-x

US EPA (1999) Determination of volatile organic compounds in ambient air using active sampling onto sorbent tubes, compendium of methods for the determination of toxic organic compounds in ambient air, 2nd Edition Compendium Method TO-17, U.S. Environmental Protection Agency (US EPA), Washington, DC

Valencia A, Muñiz-Valencia R, Ceballos-Magaña SG, Rojas-Mayorga CK, Bonilla-Petriciolet A, González J, Aguayo-Villarreal IA (2022) Cyclohexane and benzene separation by fixed-bed adsorption on activated carbons prepared from coconut shell. Environ Technol Innov 25:102076. https://doi.org/10.1016/j.eti.2021.102076

Wei M, Yu Q, Mu T, Hou L, Zuo Z, Peng J (2016) Preparation and characterization of waste ion-exchange resin-based activated carbon for CO_2 capture. Adsorption 22:385–396. https://doi.org/10.1007/s10450-016-9787-8

World Health Organization (2010) WHO guidelines for indoor air quality: selected pollutants. World Health Organization. Regional Office for Europe

Xiang Z, Tang N, Jin X, Gao W (2022) Fabrications and applications of hemicellulose-based bio-adsorbents. Carbohydr Polym 278:118945. https://doi.org/10.1016/j.carbpol.2021.118945

Xue H, Wang X, Xu Q, Dhaouadi F, Sellaoui L, Seliem MK, Lamine AB, Belmabrouk H, Bajahzar A, Bonilla-Petriciolet A, Li Z, Li Q (2022) Adsorption of methylene blue from aqueous solution on activated carbons and composite prepared from an agricultural waste biomass: a comparative study by experimental and advanced modeling analysis. Chem Eng J 430:132801. https://doi.org/10.1016/j.cej.2021.132801

Yang X, Yi H, Tang X, Zhao S, Yang Z, Ma Y, Feng T, Cui X (2018) Behaviors and kinetics of toluene adsorption-desorption on activated carbons with varying pore structure. J Environ Sci 67:104–114. https://doi.org/10.1016/j.jes.2017.06.032

Yang R, Zhou J, Wu L, Ping S (2022) Fabrication of developed porous carbon derived from bluecoke powder by microwave-assisted KOH activation for simulative organic wastewater treatment. Diam Relat Mater 124:108929. https://doi.org/10.1016/j.diamond.2022.108929

Yao L, Chu B, Wang J, Wang M (2023) Atmospheric chemistry in the urban air. Front Environ Sci 11:266. https://doi.org/10.3389/fenvs.2023.1166400

Yu Q, Zhao H, Zhao H, Sun S, Ji X, Li M, Wang Y (2019) Preparation of tobacco-stem activated carbon from using response surface methodology and its application for water vapor adsorption in solar drying system. Sol Energy 177:324–336. https://doi.org/10.1016/j.solener.2018.11.029

Zavala M, Brune WH, Velasco E, Retama A, Cruz-Alavez LA, Molina LT (2020) Changes in ozone production and VOC reactivity in the atmosphere of the Mexico City Metropolitan Area. Atmos Environ 238:117747. https://doi.org/10.1016/j.atmosenv.2020.117747

Zhang X, Gao B, Creamer AE, Cao C, Li Y (2017) Adsorption of VOCs onto engineered carbon materials: a review. J Hazard Mater 338:102–123. https://doi.org/10.1016/j.jhazmat.2017.05.013

Zhang R, Zeng L, Wang F, Li X, Li Z (2022) Influence of pore volume and surface area on benzene adsorption capacity of activated carbons in indoor environments. Build Environ 216:109011. https://doi.org/10.1016/j.buildenv.2022.109011

Zhao J, Yu L, Ma H, Zhou F, Yang K, Wu G (2020) Corn stalk-based activated carbon synthesized by a novel activation method for high-performance adsorption of hexavalent chromium in aqueous solutions. J Colloid Interface Sci 578:650–659. https://doi.org/10.1016/j.jcis.2020.06.031

Zhao Z, Pei Y, Zhao P, Wu C, Qu C, Li W, Zhao Y, Liu J (2022) Characterizing key volatile pollutants emitted from adhesives by chemical compositions, odor contributions and health risks. Molecules 27(3):1125. https://doi.org/10.3390/molecules27031125

Zhu L, Shen D, Luo KH (2020) A critical review on VOCs adsorption by different porous materials: species, mechanisms and modification methods. J Hazard Mater 389:122102. https://doi.org/10.1016/j.jhazmat.2020.122102